

Published in final edited form as:

Cell Metab. 2012 December 5; 16(6): 765–776. doi:10.1016/j.cmet.2012.10.016.

Adipose-Specific Deletion of TFAM Increases Mitochondrial Oxidation and Protects Mice against Obesity and Insulin Resistance

Cecile Vernochet¹, Arnaud Mourier², Olivier Bezy^{1,6}, Yazmin Macotella^{1,7}, Jeremie Boucher¹, Matthew J. Rardin³, Ding An¹, Kevin Y. Lee¹, Olga R. Ilkayeva⁴, Cristina M. Zingaretti⁵, Brice Emanuelli¹, Graham Smyth¹, Saverio Cinti⁵, Christopher B. Newgard⁴, Bradford W. Gibson³, Nils-Göran Larsson², and C. Ronald Kahn¹

¹Section on Integrative Physiology and Metabolism, Joslin Diabetes Center and Department of Medicine, Harvard Medical School, Boston, MA

²Max Planck Institute for Biology of Ageing, Robert-Koch-Str. 21, 50931 Cologne, Germany

³Buck Institute for Research on Aging, 8001 Redwood Boulevard, Novato, CA 94945, USA

⁴Sarah W. Stedman Nutrition and Metabolism Center, Duke University Medical Center, Durham, NC 27704, USA

⁵Department Experimental and Clinical Medicine-Diagnostic Electron Microscopy Unit University-United Hospitals of Ancona, Ancona 60020 & Adipose Organ Lab IRCCS San Raffaele Pisana, Rome 00163, Italy

⁶Pfizer, Inc, Cardiovascular Metabolic and Endocrine Diseases (CVMED), 620 Memorial Drive, Cambridge, MA 02139

⁷Instituto de Neurobiología, Universidad Nacional Autónoma de México (UNAM), Campus UNAM-Juriquilla, 76230 Querétaro, Mexico.

Abstract

Obesity and type 2 diabetes are associated with mitochondrial dysfunction in adipose tissue, but the role for adipose tissues mitochondria in the development of these disorders is currently unknown. To understand the impact of adipose tissue mitochondria on whole body metabolism, we have generated a mouse model with disruption of the mitochondrial transcription factor A (TFAM) specifically in fat. F-TFKO adipose tissue exhibit decreased mtDNA copy number, altered levels of proteins of the electron transport chain, and perturbed mitochondrial function with decreased Complex I activity and greater oxygen consumption and uncoupling. As a result, F-TFKO mice exhibit higher energy expenditure and are protected from age- and diet-induced obesity, insulin resistance and hepatosteatosis, despite a greater food intake. Thus, TFAM deletion in the adipose tissue increases mitochondrial oxidation that has positive metabolic effects suggesting that regulation of adipose tissue mitochondria may be a potential therapeutic target for the treatment of obesity.

© 2012 Elsevier Inc. All rights reserved.

^{*}To whom correspondence should be addressed: C. Ronald Kahn, MD, Joslin Diabetes Center, 1 Joslin Place, Phone: (617) 732-2635, Fax: (617) 732-2593, c.ronald.kahn@joslin.harvard.edu.

Publisher's Disclaimer: This is a PDF file of an unedited manuscript that has been accepted for publication. As a service to our customers we are providing this early version of the manuscript. The manuscript will undergo copyediting, typesetting, and review of the resulting proof before it is published in its final citable form. Please note that during the production process errors may be discovered which could affect the content, and all legal disclaimers that apply to the journal pertain.

Keywords

Obesity; Brown adipose tissue; Mitochondrial function; mitochondrial bioenergetics; White adipose tissue; Insulin resistance; Diabetes

Introduction

Obesity has reached epidemic proportions worldwide leading to numerous co-morbidities, including high rates of type 2 diabetes and metabolic syndrome, accelerated cardiovascular disease and increased cancer risk (Haslam and James, 2005). While reducing caloric intake is the first line of defense against obesity, an alternative strategy would be to modify the metabolic efficiency and increase energy expenditure in key metabolic organs, such as adipose tissue.

The function of both types of adipose tissue, white adipose tissue (WAT) and brown adipose tissue (BAT), depends on mitochondria activity (Vernochet et al., 2010; Kusminski and Scherer, 2012). BAT contains numerous mitochondria involved in fatty acid β -oxidation and specifically expresses uncoupling protein 1 (UCP1) that allows a mitochondrial electron leak producing energy expenditure through thermogenesis (Ricquier, 2005). WAT contains fewer mitochondria than BAT, but its mitochondria are crucial to adipogenic differentiation (Villarroya et al., 2009) and are essential to maintain white adipocyte functions, including normal adipokine secretion (Koh et al., 2007; Kusminski and Scherer, 2012).

Mitochondrial dysfunction in adipose tissue has been reported in HIV-1-infected patients undergoing anti-retroviral treatment (Giralt et al., 2011), as well as in obesity, type 2 diabetes and the metabolic syndrome (reviewed in (Patti and Corvera, 2010)). Mitochondrial DNA (mtDNA) copy number, mitochondrial mass and mitochondrial activity are all decreased in the white adipose tissue of mouse models of obesity, such as ob/ob and db/db mice (Choo et al., 2006; Rong et al., 2007). In humans, there is a downregulation of the expression and activity of components of oxidative phosphorylation (OXPHOS) in white adipose tissue that correlates with the level of obesity, while a lower mtDNA copy number is associated with type 2 diabetes (Dahlman et al., 2006; Kaaman et al., 2007). The mitochondrial dysfunction, which could impair substrate oxidation in adipose tissue, is thought to participate in metabolic impairment capacity, thereby accentuating the development of obesity and associated pathologies, such as type 2 diabetes.

The major function of mitochondria, and a common area of dysfunction, is the production of ATP through the mitochondrial electron transport chain (ETC) and the ATP synthase, which together are composed of ~90 proteins that form five complexes controlling oxidative phosphorylation (OXPHOS) (Gaspari et al., 2004). 13 OXPHOS proteins are mitochondrial-encoded and, although only a minority, are required for proper mitochondrial function. Fatty acids and pyruvate are metabolized in the mitochondrion to feed the tricarboxylic acid (TCA) cycle thereby generating a gradient of protons leading to increased mitochondrial membrane potential and the consumption of oxygen. In all cells, including adipocytes, this energy gradient is then converted into ATP by the F1F0-ATPase. In BAT, this energy gradient can also be converted to heat through the action of uncoupling protein 1 (UCP1) (Jastroch et al., 2010).

Mitochondrial transcription factor A (TFAM) is necessary for mtDNA stability and also initiates mtDNA transcription that is essential for mtDNA replication and mitochondrial-encoded gene transcription (Gaspari et al., 2004). Global deletion of TFAM is

embryonically lethal (Larsson et al., 1998), illustrating the important role of TFAM in mtDNA transcription and replication.

To better understand the impact of mitochondria on adipose tissue function, we have selectively disrupted TFAM in brown and white adipose tissues of the mouse using Cre-lox-mediated recombination. We find that reducing TFAM in adipose tissue increases mitochondria oxidation capacity due to complex I deficiency and greater uncoupling. The resultant F-TFKO mice are protected from age- and diet-induced obesity, glucose intolerance and hepatosteatosis through increased energy expenditure.

Results

TFAM is efficiently deleted in both the white and brown adipose tissues in F-TFKO mice

Mitochondria play an important role in both brown and white adipose tissue (Ahima, 2006; Farmer, 2008). As expected, mRNA (Figure S1A, left panel) and protein (Figure 1A) for the mitochondrial transcription factor TFAM was more highly expressed in interscapular brown adipose tissue (BAT) than in subcutaneous inguinal white adipose tissue (WAT) of adult mice. In parallel, BAT also expressed higher levels of mRNAs for mitochondrial-encoded genes, including mtATP6, mtCytb, and mtCo1 (Figure S1A, right panel).

To investigate the impact of mitochondria function in fat, we created animals with adipose-specific ablation of *TFAM* by breeding mice carrying the aP2 promoter-Cre transgene with mice carrying a floxed *TFAM* allele that contained loxP sites surrounding exons 6 and 7 (Larsson et al., 1998). The resultant aP2-Cre; *TFAM*^{fl/fl} (termed fat-specific TFAM KO or F-TFKO) mice were viable and born at a normal Mendelian ratio, but exhibited a 5-10% reduction in body length throughout life (Figure S1B). DEXA scans at 2 months of age confirmed an 8.5% reduction in femur length and a parallel reduction in lean body mass which was reflected in individual muscle weights (Figure S1C).

WAT is composed of white adipocytes, but also others cell types that comprise the stromal vascular fraction (SVF). Since white adipocytes contain fewer mitochondria than brown adipocytes and cells of the SVF can contribute significantly to properties of the whole tissue (Figure S1D-E), for most studies of WAT, we isolated mitochondria from the purified adipocyte fraction of inguinal WAT (termed white adipocytes or AF WAT, hereafter). Brown adipocytes, on the other hand, are very rich in mitochondria, and BAT contains fewer SVF cells, so that this tissue could be studied without cell fractionation. Western blots revealed a 58% and 81% reduction in TFAM protein in respectively, F-TFKO white adipocytes and BAT compared to control (Figure 1A). These changes in protein were paralleled by 64% and 52% decreases in TFAM mRNA by qPCR in F-TFKO white adipocytes and BAT (Figure 1B). Recombination was not efficient in perigonadal fat at this age (Figure S1F). In inguinal WAT, the knockout was specific to adipocytes; no differences in TFAM mRNA levels were found in macrophages isolated from the peritoneal cavity or from SVF, or other major metabolic tissues (Figure S1G).

As a result of the decrease in TFAM, the transcription of mitochondrially-encoded genes, such as mtATP6, mtCytb and mtCo1, was decreased in both F-TFKO BAT (Figure 1B, upper panel) and isolated white adipocytes (Figure 1B, lower panel). Also, mitochondrial DNA copy number was reduced by 55% in BAT and 76% in the AF-WAT (Figure 1C). By electron microscopy (EM), mitochondria from F-TFKO BAT displayed irregular shapes and disrupted cristae, while mitochondria from F-TFKO inguinal WAT showed no apparent abnormalities (Figure 1D). Morphometry analysis of EM pictures (Figure S1H) and flow cytometry analysis of isolated mitochondria (Figure S1I) revealed a significant increase in WAT mitochondrial mass in F-TFKO mice. Furthermore, white adipocyte mitochondria

were aggregated as shown by both EM (Figure S1J) and confocal microscopy (Figure S1K), and occupied 2.4-fold greater cytoplasmic area than in control WAT (Figure S1L). Thus, aP2-Cre produces efficient TFAM KO in inguinal WAT and BAT and results in decreased mtDNA copy number, decreased mitochondrially-encoded gene expression and altered mitochondrial structure in brown and white adipocytes.

Decrease of TFAM in WAT and BAT prevents age- and diet-induced obesity

To examine adipose tissue mitochondrial function and its consequences on whole body physiology and metabolism, F-TFKO mice were studied on both standard chow diet (CD) (22% of calories from fat) and after exposure to a high fat diet (HFD) with 60% of calories from fat from age 2 to 4 months. By four months of age, F-TFKO mice on CD were 34% lighter than the controls, a difference in weight significantly greater than the 8-10% difference in length and lean mass noted above. Furthermore, while the control mice gained weight on CD and HFD with age, F-TFKO mice gained significantly less weight under both dietary regimes (Figure 2A and 2B). The F-TFKO inguinal WAT mass (as measured by dissection at the time of sacrifice) was decreased by 48% and 64% on CD and HFD, respectively, while F-TFKO BAT mass was decreased by 53% on CD (Figure S2A) and 70% on HFD (Figure S2B), even after adjusting for lean mass and body weight (Figure S1B). Reduction of WAT mass in F-TFKO mice was due primarily to significantly smaller adipocytes (Figure 2C and 2D) with a decrease in average cell diameter of 33% on CD and 64% on HFD (Figure S2C). There was no apparent increase in rates of cell death or apoptosis as assessed by western blotting for cleaved Caspase 3 (Figure S2D) or impaired fat cell differentiation program (Figure S2E-F) and mitochondria biogenesis (Figure S2G-I), as analyzed by qPCR in F-TFKO WAT and BAT.

Interestingly, mRNA (Figure S2E) and protein levels (Figure S2J) of the insulin sensitive glucose transporter Glut4 and hormone sensitive lipase (HSL) in F-TFKO WAT were higher than in controls, suggesting potential for greater glucose uptake and lipolysis. Indeed, we observed a 2-fold increase in basal and insulin-stimulated 2-deoxyglucose uptake in isolated white adipocytes from F-TFKO compared to controls (Figure 2E). In parallel, the lipogenic capacity of F-TFKO white adipocytes was enhanced (Figure S2K). Basal lipolytic rates were similar for F-TFKO mice and controls, while isoproterenol-stimulated lipolysis was increased 36% in the F-TFKO adipocytes (Figure 2F). Interestingly ¹⁴C-palmitate oxidation was increased by 49% in F-TFKO brown adipocytes and 75% in F-TFKO white adipocytes compared to their respective controls (Figure 2G).

Increased lipolysis has been associated with increased macrophage infiltration and inflammation, but we found no difference in CD11c, CD68, F4/80 and IL6 and TNF α expression between control and F-TFKO WAT (Figure S2L and S2M). Circulating levels of TNF α and IL6 were also similar between F-TFKO and control mice (Figure S2N and S2O), a further indication that TFAM KO in adipose tissue does not trigger adipose tissue and systemic inflammation. Thus, fat-specific TFAM KO mice were protected against diet-induced obesity, and F-TFKO adipocytes remain small with improved glucose uptake and lipolytic activity consistent with an enhanced insulin sensitivity state.

Decrease of TFAM in WAT and BAT prevents development of insulin resistance and increase energy expenditure

Consistent with this increased insulin sensitivity, significant changes in several metabolic parameters were apparent. At 4 months of age, CD and HFD fed F-TFKO mice exhibited a reduction in fasting glucose levels (Figure 3A) and in fed plasma insulin levels compared to their respective control (Figure 3B). F-TFKO mice on both the CD (Figure 3C) and HFD (Figure 3D) showed improved glucose tolerance when compared to appropriate controls. F-

TFKO mice also exhibited increased insulin sensitivity after HFD on i.p. insulin tolerance testing (Figure S3A and 3B). The F-TFKO mice were also protected from hepatosteatosis. At 4 months of age, the livers of control mice on HFD were enlarged (Figure S3C) and exhibited gross lipid accumulation (Figure S3D) and increased triglycerides content (Figure S3E), whereas the livers of the F-TFKO mice on HFD were not enlarged and showed no signs of hepatosteatosis. By 10 months of age, the body weight differences were maintained on both CD and HFD (Figure S3F), while fasting glucose levels (Figure S3G) and glucose tolerance (Figure S3I) in the F-TFKO and controls were no longer significantly different. However, the F-TFKO mice remained more insulin sensitive on HFD as indicated by a lower insulin level (Figure S3H) and improved insulin tolerance testing (Figure S3J).

Adipose tissue secretes numerous adipokines, including the insulin-sensitizing hormone adiponectin and the central regulator of food intake leptin (Klaus, 2004; Friedman, 2009). Interestingly in the F-TFKO mice, circulating adiponectin levels were reduced by 44% (Figure 3F) despite greater insulin sensitivity, whereas, consistent with the small adipocyte size and mass, circulating leptin levels were decreased by $75\pm 1\%$ ($p<0.01$) compared to controls (Figure 3L). Lower circulating adiponectin was unexpected since adiponectin mRNA (Figure S2E) and intracellular adiponectin protein levels (Figure S2J) were actually increased in F-TFKO inguinal WAT. This suggested an alteration in adiponectin secretion and/or processing. Also, circulating FFA was slightly decreased in F-TFKO mice on CD in the fed state, but were elevated upon fasting to the same extent as the controls (Figure S3K).

To better understand how F-TFKO mice remained lean, energy expenditure was measured in two month-old mice using CLAMS metabolic cages. Despite similar body weights at this age (Figure S3L), the F-TFKO mice showed 22% higher food intake (Figure 3G) and a 10% increase in oxygen consumption compared to controls (adjusted per g of lean mass; Figure 3H). VCO₂ was not changed leading to a decrease in RER (Figure S3M). Thus, the protection against obesity exhibited by F-TFKO mice was primarily due to increased energy expenditure and it was not accompanied by an increase in basal body temperature (Figure S3N) but rather a slightly higher sensitivity to short term cold exposure (Figure S3O), probably to a reduced insulation and/or reduced BAT mass.

TFAM KO remodels adipose tissue mitochondria OXPHOS function

To directly characterize the impact of the TFAM KO on adipose tissue mitochondrial function, we analyzed the relative levels of mitochondrial- and nuclear-encoded proteins involved in OXPHOS by western blotting (Figure 4A quantified in Figure S4A), mass spectroscopy-based proteomics and functional assays. As expected, there was a 60-70% decrease of the mitochondrial-encoded gene Cytochrome b (mtCytb) and mtCo1 in both the F-TFKO BAT and white adipocyte mitochondria. While mitochondria from F-TFKO BAT expressed similar levels of UCP1 protein as control mitochondria, the levels of NDUF8, a representative of complex I (CI), and subunit 1 of complex IV (CIV) were decreased in mitochondria from F-TFKO BAT and white adipocytes by 77% and 51%, respectively. By contrast, the level of Atp5A of complex V was increased in mitochondria from white adipocyte or BAT of F-TFKO mice compared to control, and succinate dehydrogenase [ubiquinone] iron-sulfur subunit (SDHB) of complex II was increased in F-TFKO white adipocyte.

Mass spectroscopic analysis of mitochondria revealed downregulation of many nuclear-encoded ETC members in the TFAM KO BAT (Figure S4B-E) except from complex II. When we grouped the mass spectroscopy results to determine whether there was systematic downregulation in any group of the respiratory chain, it appears there was systematic downregulation of proteins in complex I and complex III, relative to proteins of the “other” complexes in the respiratory chain (the results are displayed as ratios in Figure S4F and the

p-values are given in Figure S4G). Further analysis of the enzymatic function of different ETC complexes confirmed the proteomic data. There was a 42-59% decreased activity of complex I (CPLxI) and a 29-67% decreased activity of complex IV (CPLxIV) in mitochondria of F-TFKO BAT (Figure 4B) and white adipocytes (Figure 4C). By comparison, activity of complex II (CPLxII) was actually upregulated in F-TFKO BAT, and activities of complex II-III (CPLxII-III) were similar in F-TFKO and controls for BAT and white adipocytes.

Finally, we assessed citrate synthase activity, a key component of the TCA cycle, as well as control and F-TFKO WAT and BAT oxygen consumption rates (OCR). Activity of citrate synthase (CS) was increased by 18% in F-TFKO BAT and by 46% in WAT compared to control (Figure 4D). Using 10 mg pieces of WAT and BAT tissue from 2-month old in the Seahorse Flux Analyzer, we compared very similar control and F-TFKO adipose tissue in terms cellular content (Figure S4H and S4I). F-TFKO BAT basal OCR was increased by 28.4% (692 ± 35 versus 538 ± 36 pM/min) compared to control BAT in presence of 2.5 mM glucose (Figure 4E) whereas F-TFKO WAT OCR was doubled compared to that of the control (486 ± 15 pM/min versus 241 ± 26 pM/min) (Figure 4F). Interestingly, incubation with 10 mM pyruvate increased BAT and WAT OCR from control mice by $50 \pm 10\%$ and $62 \pm 13\%$, respectively, but had little effect on the adipose tissues of the F-TFKO mice. Furthermore, addition of an FCCP uncoupler increased to a higher level control adipose tissue OCR than F-TFKO adipose tissue, suggesting that the adipose tissues of the TFAM KO mouse may already be at their highest metabolic rate and/or uncoupled (Figure S4J).

TFAM KO increased mitochondrial respiratory capacity through decreased complex I activity and increased uncoupling

Similar changes were observed using C3H10T1/2 mesenchymal cell lines with TFAM knockdown (KD, TFAM-shRNA1 (shTF1) and -shRNA2 (shTF2)) were TFAM protein was downregulated by 61% and 85% respectively. Indeed, it resulted in significant decreases in the expression of mitochondrial-encoded genes (Figure 5A, bottom panel), mtDNA content (Figure S5A), while mitochondria mass was increased (Figure S5B). ATP turnover in these cells, assessed using the Seahorse flux analyzer, was decreased by 40-65% (Figure 5B) while in a 4-fold increase in proton leak was observed indicating a greater uncoupling (Figure 5C). Moreover, reactive oxygen species (ROS) level were increased in TFAM KD cell lines (Figure S5C) and it was sufficient to cause a significant increase in lipid peroxidation, a monitor of oxidative damage (Figure S5D).

To dissect the mechanism by which TFAM KO lead to increase oxygen consumption, we examined the metabolic capacity of F-TFKO isolated mitochondria using different substrates in presence of ADP (State3) and inhibitors: complex I (malate/pyruvate) and complex II (succinate/rotenone) or fatty acids, such as palmitoyl-carnitine). We also measured state 4, which represents oxygen consumption not link to ATP synthesis, i.e. respiration due to uncoupling. In the presence of complex I substrates, no difference in state 3 OCR was detected between F-TFKO and control mitochondria (Figure 5D) whereas in the presence of fatty acids, state 3 OCR was significantly higher in F-TFKO compared to control for mitochondria from both BAT and white adipocytes (Figure 5E). Moreover, in presence the of complex II substrate, OCR was also increased in BAT and white adipocyte mitochondria from F-TFKO mice by 49% and by 75%, respectively (Figure 5F), demonstrating increased metabolic flux and respiratory capacity despite complex I dysfunction. Thus, in TFAM KO mitochondria, respiratory function has shifted and relies primarily on complex II function. Calculation of respiratory control ratio ($RCR = \text{state3}/\text{state4}$), an index of mitochondrial coupling, revealed that in F-TFKO BAT and white adipocyte mitochondria, RCR was slightly but significantly lower than control and demonstrated an intrinsic chronic uncoupling (Figure 5G). TFAM deletion triggered a

greater proton leak that did not rely on UCP1 in BAT, since a lower RCR was maintained despite GDP competition (Figure S5E).

Moreover isolated mitochondrial function was assessed by flow cytometry with the accumulation of the potential-sensitive mitochondria-specific dye TMRE. Mitochondria from F-TFKO BAT and white adipocyte accumulated significantly less TMRE dye after addition of oligomycin A, a complex V (ATP synthase) inhibitor, further supporting the idea of greater proton leak in adipocytes mitochondria upon TFAM KO (Figure 5H). Sorting allowed us to select and to compare the oxygen consumption rate of only MitoTracker green/TMRE positive mitochondria and remove potential debris that might contribute to protein content. In the presence of complex II substrate, state 3 OCR of F-TFKO BAT and WAT mitochondria drastically increased by $79\pm 19\%$ and $210\pm 39\%$ respectively (Figure 5I), consistent with increased oxidative function. The combination of increased tissue, cellular and mitochondrial oxygen consumption rates, reduced RCR and TMRE accumulation following oligomycin treatment clearly indicates a greater oxidation rate and uncoupling from F-TFKO adipose tissues mitochondria.

Effects of TFAM Reduction on Adipose Tissues Metabolites

To complete the characterization of F-TFKO adipose tissue, measures of lipid and DNA oxidative damage were conducted, as well as metabolomic profiling of organic acids and acyl carnitines using a quantitative mass spectroscopic approach. As shown in Figure 6A and 6B, increased lipid peroxidation (TBARS) and oxidative DNA damage (8-hydroxydeoxyguanosine or 8OHdG) are both observed within F-TFKO WAT and BAT only upon HFD feeding and not in CD feeding condition (Figure S6A and S6B).

Metabolomic analysis revealed increased levels of almost all Krebs cycle intermediates in BAT from F-TFKO (Figure 6C) as of well as pyruvate and lactate level, such changes are most commonly associated with an increased glycolysis. Fatty acid profiling of BAT and WAT revealed higher levels of multiple acyl carnitines in the F-TFKO BAT (Figure 6C) and F-TFKO WAT (Figure 6D). Short (S) and medium chain (MC) acyl carnitines were upregulated in F-TFKO BAT, whereas several long (L) and very long (VL) chain acyl carnitines were specifically increased in adipose tissue of F-TFKO mice independently of nutritional status. These may be related to altered peroxisome biogenesis with decreased expression of PEX3 and PEX19 or function with the downregulation of β -ketothiolase enzyme (Figure S6D). This is further suggested by changes in peroxisome aggregation in white adipocytes (Figure S6E). Interestingly, a subset of these acyl carnitines, including C6, C8, C10, C10-OH/C8-DC, C22:4 in fed F-TFKO BAT and C5:1, C8:1-OH/C6:1-DC, C10:2, C7-DC, C8:1-DC in F-TFKO fed WAT were also increased in control mice upon fasting (Figure 6E and Figure 6F), suggesting they may be linked to higher rates of lipolysis. Finally, while this set of acyl carnitines was upregulated in F-TFKO BAT either in fed or fasted state they were comparable in F-TFKO fasted WAT to control fed WAT indicating a unique adaptation of WAT to TFAM deletion. Thus TFAM deletion in adipose tissues results in remodeling of the OXPHOS process and changes in glycolysis and lipid oxidation with increased ETC flux and uncoupled respiration, giving rise to more metabolically active adipose tissue (Figure 7).

Discussion

At the whole body level, proper mitochondria function is required for normal metabolism and health (Trifunovic et al., 2004; Lane, 2006). Study of genetic diseases associated with mitochondria dysfunction has revealed variability in the metabolic consequences. In general phenotypic and biochemical mitochondrial dysfunction are observed only when some threshold is exceeded (Rossignol et al., 2003), indicating that mitochondria are more

adaptable to alterations in ETC function than previously thought. Consequences of TFAM deletion on cell function are tissue specific, ranging from absence of a phenotype for epidermal progenitor cells (Baris et al., 2011) to drastic alteration of cellular viability and function for cells that rely highly on oxidative function (Silva et al., 2000; Wredenberg et al., 2006; Wang et al., 1999; Sterky et al., 2011). In the present study, we have found that reduction of TFAM in adipose tissue of mice reduces mtDNA copy and results in remodeling of the ETC through downregulation of multiple proteins involved in oxidative phosphorylation. As a result, and somewhat surprisingly, F-TFKO mice exhibit higher energy expenditure and are protected from age- and diet-induced obesity, insulin resistance and hepatosteatosis.

Inactivation of TFAM in BAT and WAT results in decreased complex I and IV enzymatic activity, which is similar to changes observed in heart and skeletal muscle following tissue-specific TFAM KO (Wang et al., 1999; Wredenberg et al., 2006). Although the association of complex IV dysfunction with normal or even increased mitochondrial respiratory function appears paradoxical, similar findings have been reported in other situations (Letellier et al., 1994; Kunz et al., 1999; Dell'agnello et al., 2007). It is thus likely that F-TFKO complex IV activity is below the threshold to produce failure of the ETC. In our system, complex I enzymatic activity is also significantly decreased in F-TFKO BAT and WAT. To compensate, ETC flux is increased in presence of complex II substrates. This is in accordance with previous human studies showing that reduction of complex I activity, showed increased oxidative capacity in presence of complex II substrate (Hoppel et al., 1987) and increased fatty acid oxidation (Roef et al., 2002). Finally patients with isolated complex I deficiency (CID) in skeletal muscle mitochondria have increased whole body oxygen consumption at rest (Roef et al., 2002). TFAM deletion in adipose tissue results in a similar effect, with a shift from complex I to complex II dependent respiratory function, an increase in citrate synthase activity and basal respiratory capacity.

Moreover, *in vitro* knockdown of TFAM increase mitochondrial membrane proton leak. The decreased respiratory control ratio (RCR) in isolated mitochondria from F-TFKO mice further confirmed a chronic and moderate uncoupled state of mitochondria from adipose tissues triggered by TFAM deletion *in vivo*. It is difficult to define how much uncoupling and increased flux contributes to the increase in oxygen consumption in the F-TFKO mice because they exhibit a shift from complex I to II driven respiration. However, based on our results, it is clear that increasing mitochondria oxidation in fat has positive metabolic effects that protect mice from obesity and insulin resistance, despite lower circulating adiponectin level and increased adipose tissue oxidative stress .

Dysregulation of electron transport chain function is present in many insulin resistant states, including type 2 diabetes and obesity (Keller and Attie, 2010). In humans, downregulation of OXPHOS genes in skeletal muscle is associated with insulin resistance (Patti et al., 2003). Impairment of mitochondrial biogenesis by (Handschin et al., 2007b; Handschin et al., 2007a; Vianna et al., 2006) leads to abnormal glucose homeostasis. Conversely, increased mitochondrial biogenesis in skeletal muscle has been reported to protect mice against diet-induced obesity and insulin resistance (Attane et al., 2012; Chen et al., 2010). However, skeletal muscle TFAM KO (Wredenberg et al., 2006) or AIF KO (Pospisilik et al., 2007) mice have improved glucose tolerance, similar to adipose-specific TFAM deletion. In both models, complex I and complex IV activity are downregulated and are protected from obesity even upon HFD feeding and remain insulin sensitive.

The metabolomic analysis adds another dimension to the role of normal mitochondrial function in adipose tissue. This revealed an accumulation of pyruvate and lactate in F-TFKO BAT consistent with increased glycolysis. Similar effects are seen in heart after TFAM KO,

as a metabolic switch triggers greater rates of glycolysis, probably as the result of insufficient ATP production from oxidative phosphorylation (Hansson et al., 2004). In terms of fatty acid metabolism, F-TFKO adipocytes have increased FA oxidation capacity, but there are also a upregulation of two specific sets of acyl carnitines – one which mirrors the effects of fasting and one which is independent of fasting – giving TFAM KO adipose tissue a unique metabolic signature.

Strategies to combat obesity and improve insulin sensitivity include increasing BAT mass and/or activity, and “browning” of white adipose tissue (Cao et al., 2011; Bostrom et al., 2012; Fisher et al., 2012; Bordicchia et al., 2012; Vernochet et al., 2010). The latter is a term used to describe an increase in mitochondrial number and induction of BAT markers, such as UCP1, Cidea, and diiodinase 2, in WAT (Tseng et al., 2010). Another approach to combat obesity and improve insulin sensitivity would be to increase energy expenditure of white adipose or other tissues by promoting futile cycle activity through enhancing uncoupled respiration (Harper et al., 2008; Colman, 2007; De et al., 2009). This raises the possibility of developing safer chemical uncouplers that could be used to treat obesity by increasing mitochondria oxidation rate either by lowering the coupling efficiency and/or increasing ETC flux through complex 1 deficiency. Interestingly, TZDs and Metformin have been shown to inhibit complex I activity (Brunmair et al., 2004) and both of them are used for the treatment of type 2 diabetes as they improve glucose metabolism. Whether agents that reduce levels of TFAM in adipose tissue could be another possibility remains to be determined but regulation of mitochondrial function in adipose tissue and/or muscle may be a potential therapeutic target for the treatment of obesity and type 2 diabetes.

Material and Methods

Animals and Diets

aP2-Cre transgenic (Abel et al., 2001) and *TFAM* floxed (*TFAM^{f/f}*) mice (Larsson et al., 1998) have previously been described. Animal care and study protocols were approved by the Animal Care Committee of Joslin Diabetes Center. Maintenance of mice is described in detail in the Supplemental Experimental Procedures.

Body composition and metabolic analysis

Body composition was measured using a Lunar PIXImus2 densitometer (GE Medical Systems). Activity was measured using the OPTO-M3 sensor system (Comprehensive Laboratory Animal Monitoring System, CLAMS; Columbus Instruments). Indirect calorimetry was measured on the same mice using an open-circuit Oxymax system (Columbus Instruments). For metabolic cage analysis, two separate groups of mice were utilized. The first group was composed of two-month old mice fed a chow diet *ad libitum* (7 F-TFKO and of 6 control Lox). The second group was composed of 7 five-month old F-TFKO and 8 control mice fed either a chow diet or high fat diet *ad libitum* (starting 6 weeks of age). The detailed methods and calculation are described in the Supplemental Experimental Procedures.

Intraperitoneal glucose (2 g/kg weight) and insulin tolerance (1.25 unit/kg) tests were performed after a 16- and 4-h fast, respectively. Insulin, free fatty acids, leptin, adiponectin were measured by ELISA (Crystal Chem). Further details can be found in the Supplemental Experimental Procedures.

Cell Culture

Tfam was stably knocked-down in C3H10T1/2 cells by shRNA delivered by lentiviral infection. Target sets consisting of 2 separate shRNA (shTF1 and shTF2) sequences for each

gene cloned into pLKO.1. A pool of shRNA against *TFAM* (RMM4534-NM_009360) as well as shSCR in pLKO.1 was purchased from Open Biosystems. Cell culture procedures can be found in the Supplemental Experimental Procedures.

Analysis of Gene Expression and mtDNA by Quantitative PCR

Total RNA was isolated using an RNeasy minikit (Qiagen) and cDNA was synthesized with the High Capacity cDNA Reverse Transcription Kit (Applied Biosystems). Gene expression method was determined by RT-qPCR performed on a ABI Prism 7900HT sequence and provided, with primers sequences, in Supplemental Experimental Procedures.

Adipocyte Isolation and Analysis

Inguinal WAT and interscapular BAT from mice either fed a chow diet for 20 weeks or a HFD for 14 weeks (started at 6 weeks of age) (n = 4/group) were fixed in 10% formalin and embedded in paraffin and stained with hematoxylin and eosin. Adipocyte diameters were calculated using Image J software.

Adipocyte isolation, glucose uptake, lipogenesis, lipolysis and Fatty acid oxidation were measured from 10-12 weeks old control (Lox) and F-TFKO mice and are detailed in the Supplemental Experimental Procedures.

Confocal microscopy, electron microscopy and morphometric analysis

White adipocytes from F-TFKO and control mice were isolated and mitochondria were labeled using the mitochondria-specific dyes using MitoTracker Green from Molecular Probes (15 nM) for 30 min. Technical and quantification methods can be found in the Supplemental Experimental Procedures.

Western Blot Analysis

Proteins were extracted from total tissues or isolated mitochondria from white adipocytes and BAT and homogenized in 1X RIPA buffer containing 0.1% SDS. Uses of various antibodies used for immunoblotting and quantification are described in detail in the Supplemental Experimental Procedures.

Mitochondrial Analysis

F-TFKO and control mitochondria from inguinal white isolated adipocytes and interscapular BAT were isolated, analyzed by flow cytometry and sorted for further assessment of their bioenergetics profile (State 3 and RCR). Proteomic analysis and ETC activity are also further described in Supplemental Experimental Procedures

Oxidative Damage

Thiobarbituric acid reactive substances (TBARS) and 8-hydroxy-2-guanosine (8-OH-dG) methods are described in Supplemental Experimental Procedures.

Metabolomics and Lipid Analysis from Tissue and Plasma

Control and F-TFKO mice were subjected for 6 weeks to a HFD beginning 6 weeks of age. Mice were subjected or not to a 12 hours fasting before being sacrificed. Acylcarnitines and organic acids were analyzed as described in Supplemental Experimental Procedures.

Cellular and Tissue Metabolic Rate

Cellular and adipose tissue bioenergetics profile are described in details in Supplemental Experimental Procedures.

Triglycerides Quantification

Liver triglycerides content were determined with Triglyceride Colorimetric Assay kit (Cayman Chemical, Ann Arbor, MI) from 4 months old male mice on CD or HFD and details are provided in Supplemental Experimental Procedures.

Statistics

Data are expressed as means \pm SEM unless otherwise indicated. All differences were analyzed by a Student's t-test. Results were considered significant if either * $p < 0.05$ or ** $p < 0.01$.

Supplementary Material

Refer to Web version on PubMed Central for supplementary material.

Acknowledgments

The authors are grateful to Alison Burkart for helpful discussion and manuscript editing; Siegfried Ussar, for help with mitochondria isolation; Michael Rourk for animal care; Chris Cahill for confocal microscopy assistance (Joslin Diabetes Microscopy Core, P30 DK36836 and NIH S10-RR025545); Girijesh Buruzula and Joyce LaVecchio for flow cytometry assistance; Alan Clermont (DERC Physiology Core); H. Li (DERC Specialized Assay Core). This work was supported by NIH grant DK-082659, a grant from the Eli Lilly Foundation, by European Community's FP7, Grant Health-F2-2011-278373 to SC and the Mary K. Iacocca Professorship.

References

- Abel ED, Peroni O, Kim JK, Kim YB, Boss O, Hadro E, Minnemann T, Shulman GI, Kahn BB. Adipose-selective targeting of the GLUT4 gene impairs insulin action in muscle and liver. *Nature*. 2001; 409:729–733. [PubMed: 11217863]
- Ahima RS. Adipose tissue as an endocrine organ. *Obesity (Silver. Spring.)*. 2006; 14(Suppl 5):242S–249S. [PubMed: 17021375]
- Attane C, Foussal C, Le GS, Benani A, Daviaud D, Wanecq E, Guzman-Ruiz R, Dray C, Bezaire V, Rancoule C, Kuba K, Ruiz-Gayo M, Levade T, Penninger J, Burcelin R, Penicaud L, Valet P, Castan-Laurell I. Apelin treatment increases complete Fatty Acid oxidation, mitochondrial oxidative capacity, and biogenesis in muscle of insulin-resistant mice. *Diabetes*. 2012; 61:310–320. [PubMed: 22210322]
- Baris OR, Klose A, Kloepper JE, Weiland D, Neuhaus JF, Schauen M, Wille A, Muller A, Merkwirth C, Langer T, Larsson NG, Krieg T, Tobin DJ, Paus R, Wiesner RJ. The mitochondrial electron transport chain is dispensable for proliferation and differentiation of epidermal progenitor cells. *Stem Cells*. 2011; 29:1459–1468. [PubMed: 21780252]
- Bordicchia M, Liu D, Amri EZ, Ailhaud G, Dessi-Fulgheri P, Zhang C, Takahashi N, Sarzani R, Collins S. Cardiac natriuretic peptides act via p38 MAPK to induce the brown fat thermogenic program in mouse and human adipocytes. *J. Clin. Invest*. 2012; 122:1022–1036. [PubMed: 22307324]
- Bostrom P, Wu J, Jedrychowski MP, Korde A, Ye L, Lo JC, Rasbach KA, Bostrom EA, Choi JH, Long JZ, Kajimura S, Zingaretti MC, Vind BF, Tu H, Cinti S, Hojlund K, Gygi SP, Spiegelman BM. A PGC1-alpha-dependent myokine that drives brown-fat-like development of white fat and thermogenesis. *Nature*. 2012; 481:463–468. [PubMed: 22237023]
- Brunmair B, Staniek K, Gras F, Scharf N, Althaym A, Clara R, Roden M, Gnaiger E, Nohl H, Waldhausl W, Fornsinn C. Thiazolidinediones, like metformin, inhibit respiratory complex I: a common mechanism contributing to their antidiabetic actions? *Diabetes*. 2004; 53:1052–1059. [PubMed: 15047621]
- Cao L, Choi EY, Liu X, Martin A, Wang C, Xu X, Durning MJ. White to brown fat phenotypic switch induced by genetic and environmental activation of a hypothalamic-adipocyte axis. *Cell Metab*. 2011; 14:324–338. [PubMed: 21907139]

- Chen W, Zhang X, Birsoy K, Roeder RG. A muscle-specific knockout implicates nuclear receptor coactivator MED1 in the regulation of glucose and energy metabolism. *Proc. Natl. Acad. Sci. U. S. A.* 2010; 107:10196–10201. [PubMed: 20479251]
- Choo HJ, Kim JH, Kwon OB, Lee CS, Mun JY, Han SS, Yoon YS, Yoon G, Choi KM, Ko YG. Mitochondria are impaired in the adipocytes of type 2 diabetic mice. *Diabetologia.* 2006; 49:784–791. [PubMed: 16501941]
- Colman E. Dinitrophenol and obesity: an early twentieth-century regulatory dilemma. *Regul. Toxicol. Pharmacol.* 2007; 48:115–117. [PubMed: 17475379]
- Dahlman I, Forsgren M, Sjogren A, Nordstrom EA, Kaaman M, Naslund E, Attersand A, Arner P. Downregulation of electron transport chain genes in visceral adipose tissue in type 2 diabetes independent of obesity and possibly involving tumor necrosis factor-alpha. *Diabetes.* 2006; 55:1792–1799. [PubMed: 16731844]
- De PA, Tejerina S, Raes M, Keijer J, Arnould T. Mitochondrial (dys)function in adipocyte (de)differentiation and systemic metabolic alterations. *Am. J. Pathol.* 2009; 175:927–939. [PubMed: 19700756]
- Dell'agnello C, Leo S, Agostino A, Szabadkai G, Tiveron C, Zulian A, Prella A, Roubertoux P, Rizzuto R, Zeviani M. Increased longevity and refractoriness to Ca(2+)-dependent neurodegeneration in Surf1 knockout mice. *Hum. Mol. Genet.* 2007; 16:431–444. [PubMed: 17210671]
- Farmer SR. Molecular determinants of brown adipocyte formation and function. *Genes. Dev.* 2008; 22:1269–1275. [PubMed: 18483216]
- Fisher FM, Kleiner S, Douris N, Fox EC, Mepani RJ, Verdeguer F, Wu J, Kharitononkov A, Flier JS, Maratos-Flier E, Spiegelman BM. FGF21 regulates PGC-1alpha and browning of white adipose tissues in adaptive thermogenesis. *Genes Dev.* 2012; 26:271–281. [PubMed: 22302939]
- Friedman JM. Leptin at 14 y of age: an ongoing story. *Am. J. Clin. Nutr.* 2009; 89:973S–979S. [PubMed: 19190071]
- Gaspari M, Larsson NG, Gustafsson CM. The transcription machinery in mammalian mitochondria. *Biochim. Biophys. Acta.* 2004; 1659:148–152. [PubMed: 15576046]
- Giralt M, Domingo P, Villarroya F. Adipose tissue biology and HIV-infection. *Best. Pract. Res. Clin. Endocrinol. Metab.* 2011; 25:487–499. [PubMed: 21663842]
- Handschin C, Chin S, Li P, Liu F, Maratos-Flier E, LeBrasseur NK, Yan Z, Spiegelman BM. Skeletal muscle fiber-type switching, exercise intolerance, and myopathy in PGC-1alpha muscle-specific knock-out animals. *J. Biol. Chem.* 2007a; 282:30014–30021. [PubMed: 17702743]
- Handschin C, Choi CS, Chin S, Kim S, Kawamori D, Kurpad AJ, Neubauer N, Hu J, Mootha VK, Kim YB, Kulkarni RN, Shulman GI, Spiegelman BM. Abnormal glucose homeostasis in skeletal muscle-specific PGC-1alpha knockout mice reveals skeletal muscle-pancreatic beta cell crosstalk. *J. Clin. Invest.* 2007b; 117:3463–3474. [PubMed: 17932564]
- Hansson A, Hance N, Dufour E, Rantanen A, Hultenby K, Clayton DA, Wibom R, Larsson NG. A switch in metabolism precedes increased mitochondrial biogenesis in respiratory chain-deficient mouse hearts. *Proc. Natl. Acad. Sci. U. S. A.* 2004; 101:3136–3141. [PubMed: 14978272]
- Harper ME, Green K, Brand MD. The efficiency of cellular energy transduction and its implications for obesity. *Annu Rev. Nutr.* 2008; 28:13–33. [PubMed: 18407744]
- Haslam DW, James WP. Obesity. *Lancet.* 2005; 366:1197–1209. [PubMed: 16198769]
- Hoppel CL, Kerr DS, Dahms B, Roessmann U. Deficiency of the reduced nicotinamide adenine dinucleotide dehydrogenase component of complex I of mitochondrial electron transport. Fatal infantile lactic acidosis and hypermetabolism with skeletal-cardiac myopathy and encephalopathy. *J. Clin. Invest.* 1987; 80:71–77. [PubMed: 3110216]
- Jastroch M, Divakaruni AS, Mookerjee S, Treberg JR, Brand MD. Mitochondrial proton and electron leaks. *Essays Biochem.* 2010; 47:53–67. [PubMed: 20533900]
- Kaaman M, Sparks LM, van H, V, Smith SR, Sjolind E, Dahlman I, Arner P. Strong association between mitochondrial DNA copy number and lipogenesis in human white adipose tissue. *Diabetologia.* 2007; 50:2526–2533. [PubMed: 17879081]
- Keller MP, Attie AD. Physiological insights gained from gene expression analysis in obesity and diabetes. *Annu. Rev. Nutr.* 2010; 30:341–364. [PubMed: 20415584]

- Klaus S. Adipose tissue as a regulator of energy balance. *Curr. Drug Targets*. 2004; 5:241–250. [PubMed: 15058310]
- Koh EH, Park JY, Park HS, Jeon MJ, Ryu JW, Kim M, Kim SY, Kim MS, Kim SW, Park IS, Youn JH, Lee KU. Essential role of mitochondrial function in adiponectin synthesis in adipocytes. *Diabetes*. 2007; 56:2973–2981. [PubMed: 17827403]
- Kunz WS, Kuznetsov AV, Clark JF, Tracey I, Elger CE. Metabolic consequences of the cytochrome c oxidase deficiency in brain of copper-deficient Mo(vbr) mice. *J. Neurochem*. 1999; 72:1580–1585. [PubMed: 10098864]
- Kusminski CM, Scherer PE. Mitochondrial dysfunction in white adipose tissue. *Trends Endocrinol. Metab*. 2012
- Lane N. Mitochondrial disease: powerhouse of disease. *Nature*. 2006; 440:600–602. [PubMed: 16572142]
- Larsson NG, Wang J, Wilhelmsson H, Oldfors A, Rustin P, Lewandoski M, Barsh GS, Clayton DA. Mitochondrial transcription factor A is necessary for mtDNA maintenance and embryogenesis in mice. *Nat. Genet*. 1998; 18:231–236. [PubMed: 9500544]
- Letellier T, Heinrich R, Malgat M, Mazat JP. The kinetic basis of threshold effects observed in mitochondrial diseases: a systemic approach. *Biochem. J*. 1994; 302(Pt 1):171–174. [PubMed: 8068003]
- Patti ME, Butte AJ, Crunkhorn S, Cusi K, Berria R, Kashyap S, Miyazaki Y, Kohane I, Costello M, Saccone R, Landaker EJ, Goldfine AB, Mun E, DeFronzo R, Finlayson J, Kahn CR, Mandarino LJ. Coordinated reduction of genes of oxidative metabolism in humans with insulin resistance and diabetes: Potential role of PGC1 and NRF1. *Proc Natl. Acad Sci U S. A*. 2003; 100:8466–8471. [PubMed: 12832613]
- Patti ME, Corvera S. The role of mitochondria in the pathogenesis of type 2 diabetes. *Endocr. Rev*. 2010; 31:364–395. [PubMed: 20156986]
- Pospisilik JA, Knauf C, Joza N, Benit P, Orthofer M, Cani PD, Ebersberger I, Nakashima T, Sarao R, Neely G, Esterbauer H, Kozlov A, Kahn CR, Kroemer G, Rustin P, Burcelin R, Penninger JM. Targeted deletion of AIF decreases mitochondrial oxidative phosphorylation and protects from obesity and diabetes. *Cell*. 2007; 131:476–491. [PubMed: 17981116]
- Ricquier D. Respiration uncoupling and metabolism in the control of energy expenditure. *Proc. Nutr. Soc*. 2005; 64:47–52. [PubMed: 15877922]
- Roef MJ, Reijngoud DJ, Jeneson JA, Berger R, de MK. Resting oxygen consumption and in vivo ADP are increased in myopathy due to complex I deficiency. *Neurology*. 2002; 58:1088–1093. [PubMed: 11940698]
- Rong JX, Qiu Y, Hansen MK, Zhu L, Zhang V, Xie M, Okamoto Y, Mattie MD, Higashiyama H, Asano S, Strum JC, Ryan TE. Adipose mitochondrial biogenesis is suppressed in db/db and high-fat diet-fed mice and improved by rosiglitazone. *Diabetes*. 2007; 56:1751–1760. [PubMed: 17456854]
- Rosignol R, Faustin B, Rocher C, Malgat M, Mazat JP, Letellier T. Mitochondrial threshold effects. *Biochem. J*. 2003; 370:751–762. [PubMed: 12467494]
- Silva JP, Kohler M, Graff C, Oldfors A, Magnuson MA, Berggren PO, Larsson NG. Impaired insulin secretion and beta-cell loss in tissue-specific knockout mice with mitochondrial diabetes. *Nat. Genet*. 2000; 26:336–340. [PubMed: 11062475]
- Sterky FH, Lee S, Wibom R, Olson L, Larsson NG. Impaired mitochondrial transport and Parkin-independent degeneration of respiratory chain-deficient dopamine neurons in vivo. *Proc. Natl. Acad. Sci. U. S. A*. 2011; 108:12937–12942. [PubMed: 21768369]
- Trifunovic A, Wredenberg A, Falkenberg M, Spelbrink JN, Rovio AT, Bruder CE, Bohlooly Y, Gidlof S, Oldfors A, Wibom R, Tornell J, Jacobs HT, Larsson NG. Premature ageing in mice expressing defective mitochondrial DNA polymerase. *Nature*. 2004; 429:417–423. [PubMed: 15164064]
- Tseng YH, Cypess AM, Kahn CR. Cellular bioenergetics as a target for obesity therapy. *Nat. Rev. Drug Discov*. 2010; 9:465–482. [PubMed: 20514071]
- Vernochet C, McDonald ME, Farmer SR. Brown adipose tissue: a promising target to combat obesity. *Drug News Perspect*. 2010; 23:409–417. [PubMed: 20862392]

- Vianna CR, Huntgeburth M, Coppari R, Choi CS, Lin J, Krauss S, Barbatelli G, Tzameli I, Kim YB, Cinti S, Shulman GI, Spiegelman BM, Lowell BB. Hypomorphic mutation of PGC-1beta causes mitochondrial dysfunction and liver insulin resistance. *Cell Metab.* 2006; 4:453–464. [PubMed: 17141629]
- Villarroya J, Giralt M, Villarroya F. Mitochondrial DNA: an up-and-coming actor in white adipose tissue pathophysiology. *Obesity. (Silver. Spring).* 2009; 17:1814–1820. [PubMed: 19461585]
- Wang J, Wilhelmsson H, Graff C, Li H, Oldfors A, Rustin P, Bruning JC, Kahn CR, Clayton DA, Barsh GS, Thoren P, Larsson NG. Dilated cardiomyopathy and atrioventricular conduction blocks induced by heart-specific inactivation of mitochondrial DNA gene expression. *Nat. Genet.* 1999; 21:133–137. [PubMed: 9916807]
- Wredenberg A, Freyer C, Sandstrom ME, Katz A, Wibom R, Westerblad H, Larsson NG. Respiratory chain dysfunction in skeletal muscle does not cause insulin resistance. *Biochem. Biophys. Res. Commun.* 2006; 350:202–207. [PubMed: 16996481]

\$watermark-text

\$watermark-text

\$watermark-text

- Adipose tissue specific TFAM KO protects from obesity and insulin resistance
- Adipose Tissue Specific TFAM KO increases energy expenditure
- TFAM KO increases mitochondrial uncoupling and decreases Complex I activity
- Increased adipose tissue mitochondrial oxidation has positive metabolic effect

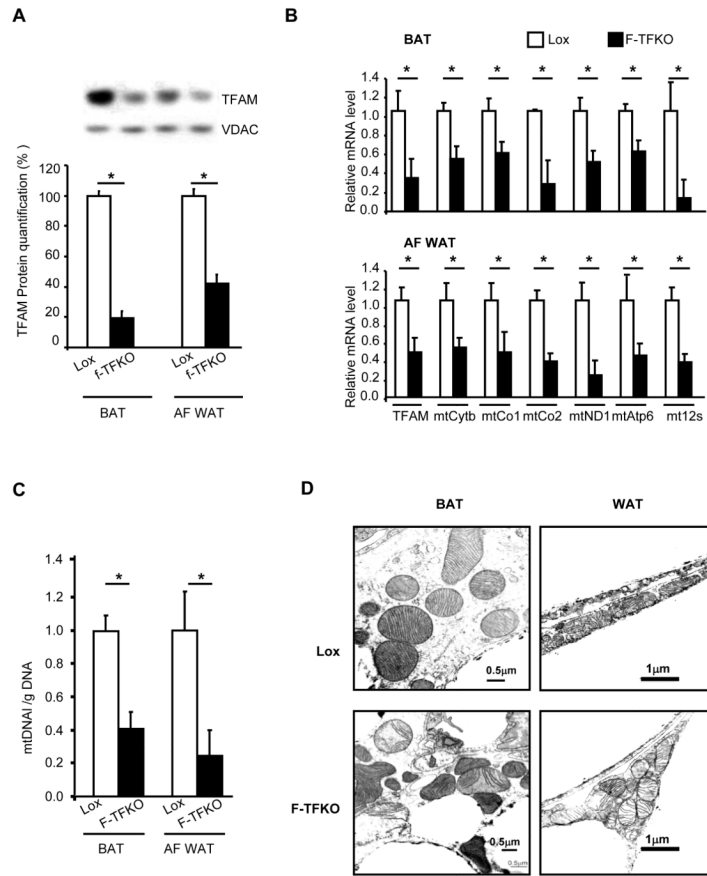


Figure 1. Effects of TFAM Knockout on Mitochondrial Gene and Protein Expression in White and Brown Adipocytes

(A) TFAM expression was analyzed by western blot in isolated mitochondria from BAT and white adipocytes (AF WAT) of Lox and F-TFKO mice at 12 weeks of age. Data are representative of 4 samples/genotype; quantification is shown in the lower panel. TFAM and mitochondrially-encoded genes mRNA levels (B) and mitochondrial DNA copy number (C) were assessed using qPCR in BAT (upper panel) and isolated white adipocytes (AF WAT) (lower panel) from 12-week-old male Lox and F-TFKO mice (n=6/genotype). (C) Mitochondria morphology of Lox and F-TFKO BAT by electron microscopy (picture representative of 5 mice /group). Values are given as mean ± SEM, * p<0.05 versus respective controls.

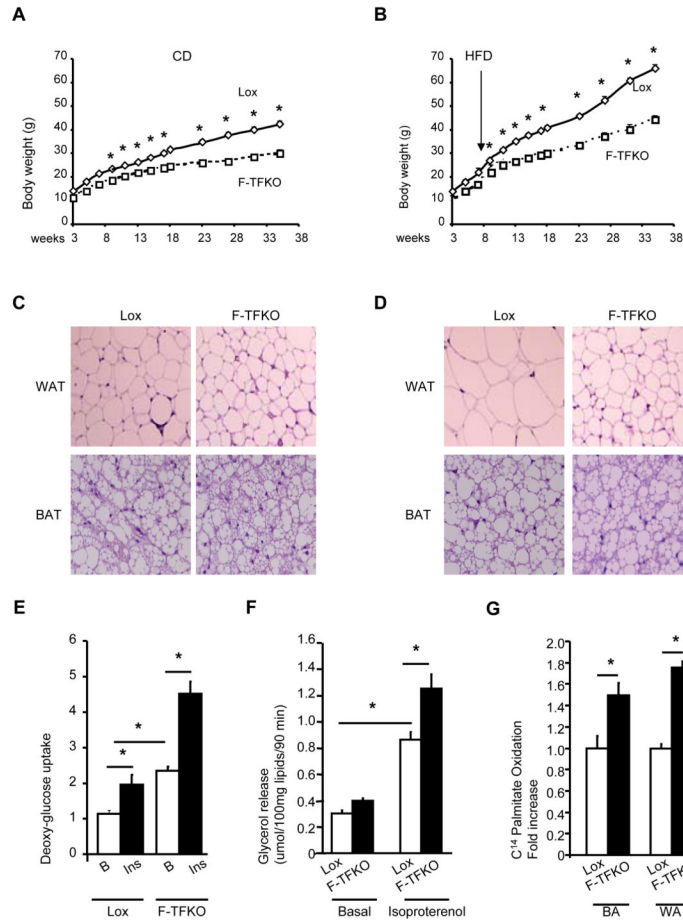


Figure 2. Ablation of *TFAM* protects mice from obesity

Body weight of male Lox and F-TFKO mice upon chow diet (CD) (A) or high fat diet (HFD) (B) (n=6/genotype/diet). Representative sections of BAT and WAT from 4 month old Lox and F-TFKO mice on CD (C) and HFD (D) (stained with hematoxylin and eosin. Pictures were taken at 20X). ³H] 2-deoxyglucose uptake (E) and glycerol release (F) for isolated white adipocytes from lox and F-TFKO animals at 12 weeks of age (n=6/genotype). (G) ¹⁴C-Palmitate oxidation by isolated brown adipocytes (BA) and white adipocytes (WA) of 10-12 weeks old lox and F-TFKO mice (n=6/genotype). Values are given as mean ± SEM, * p<0.05.

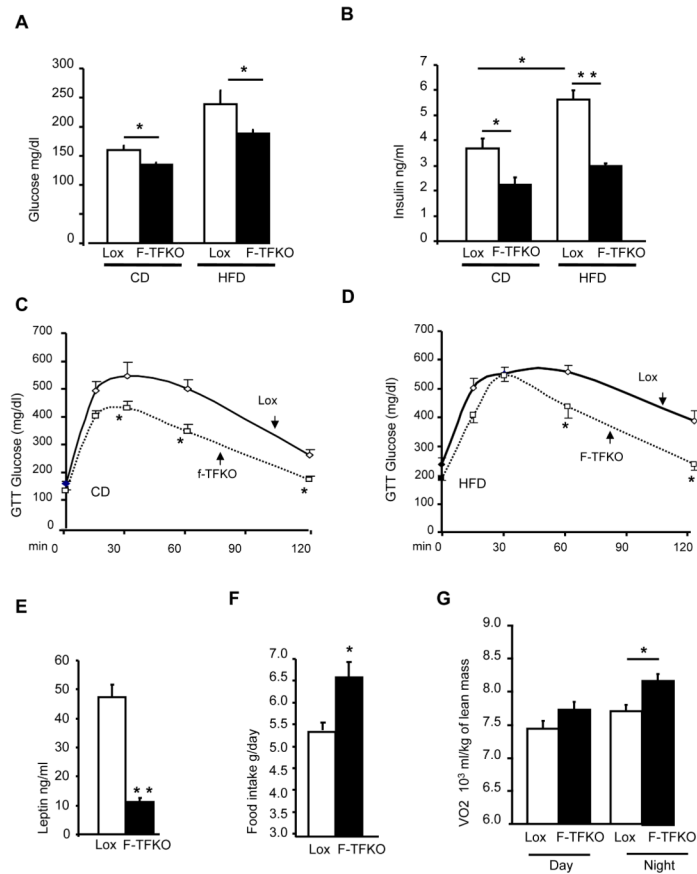


Figure 3. TFAM deletion in adipose tissue protects from insulin resistance and increases energy expenditure

Glucose level (A) and serum insulin (B) in control Lox and F-TFKO mice upon CD and HFD at 4 months of age upon fed state (n=6-8 animals/genotype/diet). Intraperitoneal glucose (C) and insulin tolerance (D) test on Lox and F-TFKO male mice on CD and HFD at 4 months of age (n=6-8 animals/genotype/diet). Leptin (E) and adiponectin (F) serum levels of Lox and F-TFKO male mice at 4 months of age (n=6-8 animals/genotype). (F) Food intake of two month old Lox and F-TFKO male mice (n=4 animals/genotype). The entire experiment was repeated twice. (G) Oxygen consumption of two month old Lox and F-TFKO male mice (n=4/genotype). The entire experiment was repeated twice. Values are given as mean \pm SEM, * p<0.05 and ** p<0.01.

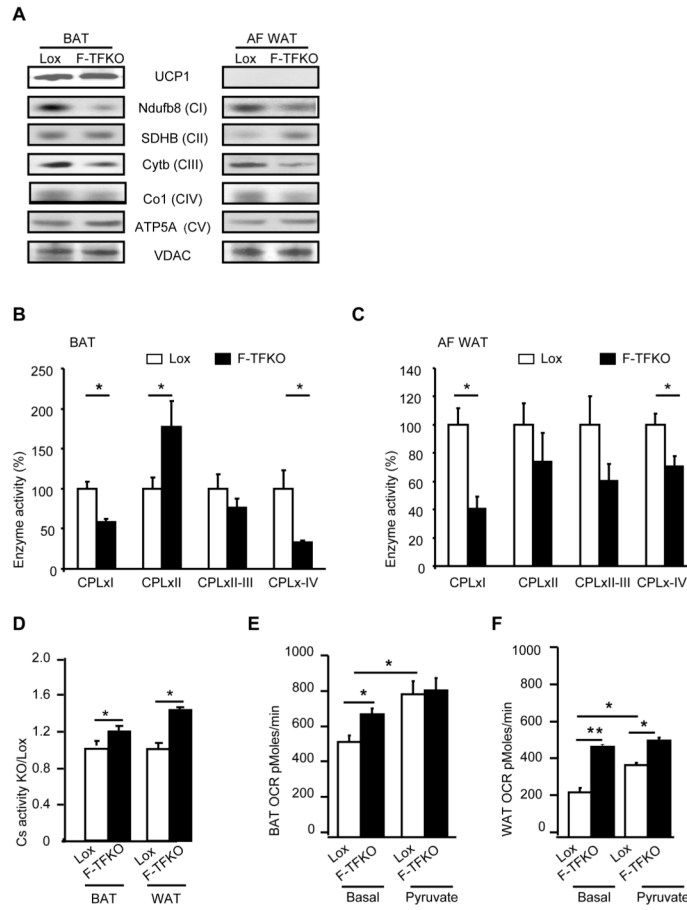


Figure 4. TFAM ablation remodels BAT and WAT mitochondria and increase adipose tissue oxygen consumption

(A) Assessment of proteins in the OXPHOS pathway by western blotting of isolated mitochondria from BAT and white adipocytes (AF WAT) of control and F-TFKO mice (8-10 weeks old). Data are representative of 4 mice per genotype and normalized in FigS9A. F-TFKO and Lox BAT (B) and white adipocyte (C) isolated mitochondria respiratory chain enzyme activities were assessed independently. Complex I (CPLxI), complex II (CPLxII), complexes II and III (CPLxII-III) and complex IV (CPLxIV) (n=6/genotype). (D) Citrate synthase activity in extracts from BAT and WAT of Lox and F-TFKO mice at 4 months of age (n=6/genotype). Oxygen consumption rate (OCR) were determined in a Seahorse X24 Flux Analyzer using pieces (10 mg) from BAT (E) and WAT (F) of Lox and F-TFKO mice under basal (2.5 mM glucose) and pyruvate (10 mM) loaded conditions. Data represent the means \pm SEM of the OCRs of 10mg from 6 adipose tissue pieces/tissue/mice from n=6/genotype * p <0.05 and ** p <0.01.

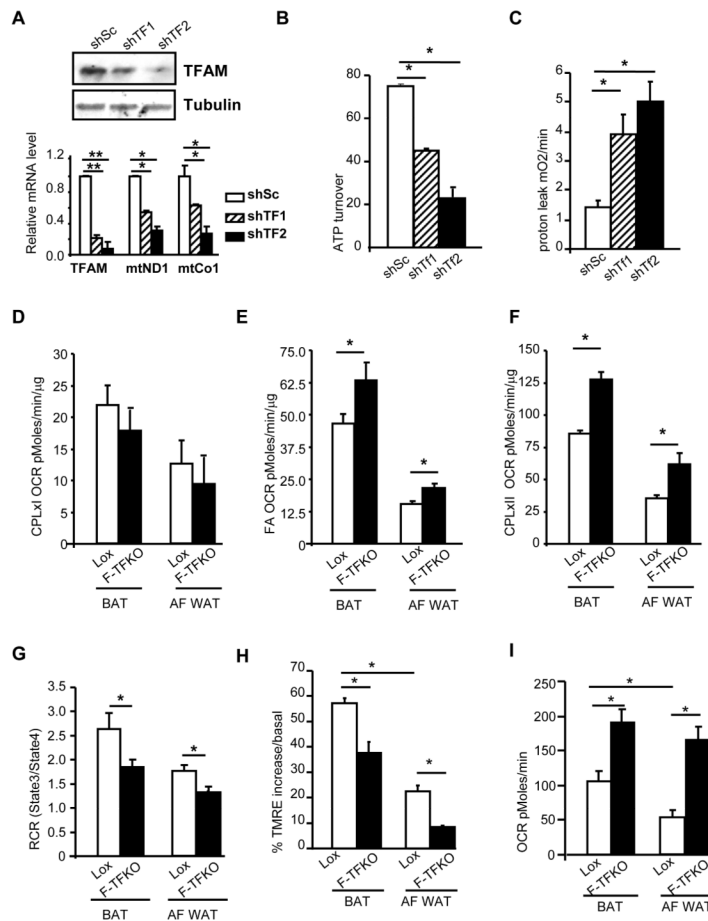


Figure 5. TFAM ablation increase adipose tissue metabolic rate through increased ETC flux and uncoupling

(A) TFAM protein levels in confluent C3H10T1/2 cells were assessed by western blot analysis (upper panel) and mRNA levels assessed by qPCR (lower panel) in the control cell line (ShSc) and 2 independent shTFAM knock down cell lines (shTF1 and shTF2). ATP turnover (B) and proton leak (C) in shTFAM C3H10T1/2 and control cell lines at confluence assessed using a Seahorse Flux Analyzer as described in Methods. (D) State 3 Respiratory rate of F-TFKO and Lox isolated mitochondria from BAT and white adipocyte (AF WAT) in presence of malate/pyruvate (complex I) and ADP from Lox and F-TFKO CD fed male mice at 10-12 weeks of age (n=9/genotype). (E) State 3 Respiratory rate of F-TFKO and Lox isolated mitochondria from BAT and white adipocyte (AF WAT) in presence of Palmitoyl-carnitine/malate (fatty acid) and ADP from Lox and F-TFKO CD fed male mice at 10-12 weeks of age (n=9/genotype). (F) State 3 Respiratory rate of F-TFKO and control isolated mitochondria from BAT and white adipocyte (AF WAT) in presence of Succinate/Glycerol-3-phosphate/rotenone (complex II) and ADP from Lox and F-TFKO CD fed male mice at 10-12 weeks of age (n=9/genotype). (G) Respiratory Control Ratio (RCR) from isolated BAT and white adipocyte (AF WAT) from Lox and F-TFKO CD fed male mice at 10-12 weeks of age in presence of complex II substrate (n=9/genotype). (H) Analysis of membrane potential of isolated mitochondria from BAT and isolated white adipocytes of control (Lox) and F-TFKO male mice based on the accumulation of the TMRE mitochondrial dye by FACS. The data are representative of the basal state and oligomycin treatment and are shown as the medians \pm SEM of n=6/genotype. (I) Oxygen consumption rate (OCR) of FACS sorted BAT and white adipocyte mitochondria were

measured using a Seahorse Flux Analyzer in presence of succinate/rotenone and ADP. The data are shown from Lox and F-TFKO CD fed male mice at 10-12 weeks of age (n=6/genotype). Values are given as mean \pm SEM, * p<0.05 and ** p<0.01.

\$watermark-text

\$watermark-text

\$watermark-text

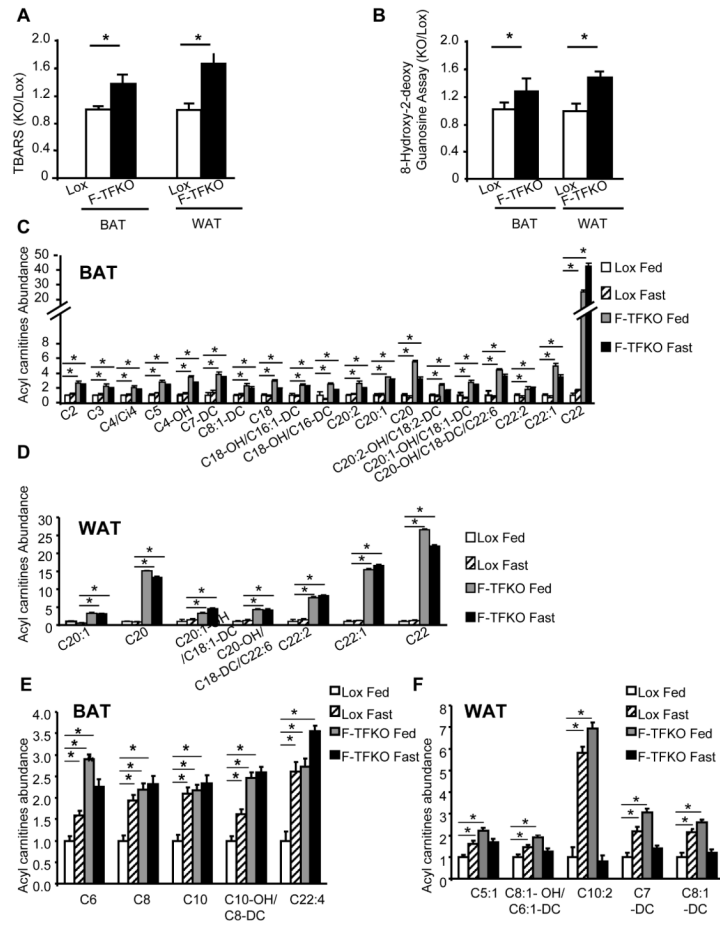


Figure 6. Adipose tissue metabolic status upon TFAM KO

Lipids peroxidation was measured by TBARS assay (A) and oxidative DNA damage was measured by 8 Hydroxy-2-deoxy guanosine (8-OHdG) (B) from F-TFKO, Lox BAT and WAT of HFD fed mice. The data are represented as fold induction compared to their respective control adipose tissue ($n=6$ /genotype). Set of Acyl carnitine levels specifically upregulated in F-TFKO BAT (C) and WAT (D) were assessed by metabolomic analysis in both fed and 24 h fasting state. Data are shown relative to Lox control fed state ($n=5$ /genotype). Acyl carnitine levels in control and F-TFKO BAT (E) and WAT (F) in fed state were analyzed by metabolomic analysis in fed and 24 h fasting state. Data are shown relative to Lox control fed state ($n=5$ /genotype), $*p < 0.05$. Asterisks indicate a significant difference in all panels ($*p < 0.05$)

\$watermark-text \$watermark-text \$watermark-text

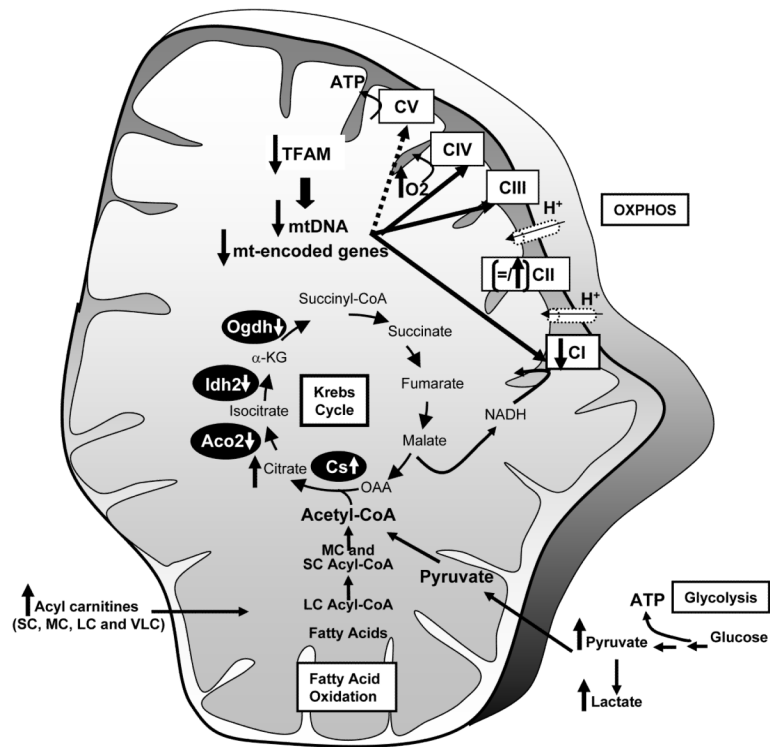


Figure 7. Schematic of changes in mitochondria of F-TFKO adipose tissue